LIVERPOOL
JOHN MOORES
UNIVERSITY

LJMU Research Online

Gao, R, Shi, Y, He, Z, Chen, Y, En, Y, Huang, Y, Ji, Z, Zhang, JF, Zhang, WD, Zheng, X, Zhang, J and Liu, Y

 A Fast Extraction Method of Energy Distribution of Border Traps in AlGaN/GaN MIS-HEMT

http://researchonline.ljmu.ac.uk/id/eprint/13479/

Article

A Fast Extraction Method of Energy Distribution of Border Traps in AlGaN/GaN MIS-HEMT

RUI GAO [1], YIJUN SHI [1], ZHIYUAN HE [1], YIQIANG CHEN [1] (Member, IEEE), YUNFEI EN [1], YUN HUANG[1], ZHIGANG JI [2] (Member, IEEE), JIANFU ZHANG [3], WEIDONG ZHANG [3], XUEFENG ZHENG[4], JINFENG ZHANG [4], AND YANG LIU[5] (Member, IEEE)

1 Science and Technology on Reliability Physics and Application of Electronic Component Laboratory, No. 5 Electronics Research Institute,
Ministry of Industry and Information Technology, Guangzhou 510610, China
2 National Key Laboratory of Science and Technology on Micro/Nano Fabrication, Shanghai Jiaotong University, Shanghai 200240, China
3 School of Engineering, John Moores University, Liverpool L3 3AF, U.K.
4 State Key Discipline Laboratory of Wide Band Gap Semiconductor Technology, School of Microelectronics, Xidian University, Xi'an 710071, China
5 School of Physics and Engineering, State Key Laboratory of Optoelectronic Materials and Technologies, Sun Yat-sen University, Guangzhou 510275, China

CORRESPONDING AUTHORS: Z. HE (e-mail: hezhiyuan1988@126.com) AND Y. CHEN (e-mail: yiqiang-chen@hotmail.com)

ABSTRACT MIS-HEMT is one of the most promising structures to prohibit the unfavorable gate leakage in conventional AlGaN/GaN HEMTs. However, the extra insulator layer introduces massive border traps at insulator/AlGaN interface and results in the poor reliability. In this brief the energy distribution of border traps in AlGaN/GaN MIS-HEMT gate stack is extracted and investigated through a discharging-based trap energy profile technique. The technique adopts spot-I_d sense measurement with 1 millisecond measurement time to capture the "whole (both fast and slow)" border traps. The results are beneficial to improve the reliability of AlGaN/GaN MIS-HEMT.
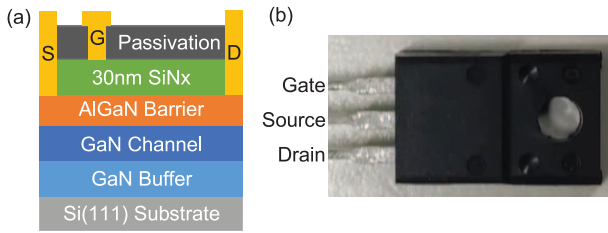
INDEX TERMS GaN MIS-HEMT, energy distribution.

I. INTRODUCTION

Owing to the large bandgap, high breakdown electric field and high saturation electron mobility, GaN has been considered as one of the most promising candidates to replace silicon, which is now approaching its physical limitation, in power electric applications. The past 3 decades witness the booming development of GaN-based high electron mobility transistors (HEMTs). Conventional AlGaN/GaN HEMTs usually suffer from the high-gate leakage, resulting in an unfavorable power loss during an OFF-state condition and a low-gate overdrive during ON-state condition. MIS-HEMT structure needs to be adopted to suppress the gate leakage. However, due to the existence of vast number of traps in the gate stack, the reliability of AlGaN/GaN MIS-HEMTs becomes one of the major concerns and precludes their commercial applications.

To improve the performance and reliability of GaN-based MIS-HEMT, energy distribution of the border traps at insulator/AlGaN interface need to be investigated.

Among the traditional characterization techniques on GaN-based HEMTs, photo-assisted techniques such as Electroluminescence (EL) characterization [1], [2] and photoionization spectroscopy [3], [4] need to heavily stress the device and will generate new traps during the measurement, thus cannot be adopted to investigate the border traps' energy distribution. Deep level transient spectroscopy (DLTS) [5], [6] mainly characterizes the deep level traps as the name suggests and the test samples need to go through repetitive CV measurements under various temperatures from cryogenic temperature to high temperature, which might also create new traps. Low frequency noise technique could probe the overall trap density [7]–[9], but the technique relies on the assumption of uniform distribution of traps in area, depth, and energy [10]. Tallarico *et al.* [11] proposed a spatial and energy distribution extraction technique of traps in p-channel of power U-MOSFETs, but the traps were characterized through slow DC I/V sweep measurements which cannot probe fast recoverable traps.

FIGURE 1. Device structure: (a) The schematic diagram of cross section and (b) photograph of the TO-247 packaged device.

FIGURE 2. Transfer characteristic and gate leakage of the device, $V_d = 0.1V$.

FIGURE 3. Test waveform of the spot-I_d sense measurement.

To the author's knowledge, the energy distribution of the border traps in AlGaN/GaN MIS-HEMT gate stack across the entire energy range has not been widely studied yet.

We have recently developed a threshold voltage shift (ΔV_{th}) based technique that can probe the energy distribution of positive charges across the whole energy domain for Si MOSFETs using fast pulse measurements [12]–[15]. Similar methodology is adopted in this work for AlGaN/GaN MIS-HEMT. Due to the power limitation of the commercial pulse measurement units, their output voltage range is usually insufficient for power devices. To make the technique more universal and applicable on mainstream semiconductor analyzer equipment such as source measure units (SMUs), a discharging-based trap energy profile (DTEP) technique is proposed in this work to overcome this output voltage range issue by replacing the fast pulse measurements with DC spot-I_d measurements, as detailed in Section II.

II. DEVICE PREPARATION

The structure of the AlGaN/GaN MIS-HEMT device used in this work is given in Fig. 1. $Al_{0.25}Ga_{0.75}N/GaN$ hetero-structure was grown on Si (111) substrate, which consists of a 25 nm $Al_{0.25}Ga_{0.75}N$ barrier layer, a 2 μm GaN buffer layer, and a GaN transition layer. A 30 nm SiN_x layer was then deposited on the AlGaN barrier layer for dielectric layer. The device has a gate length of 4 μm, a gate width of 17 mm, gate-source space of 3 μm, and gate-drain space of 15 μm. Finally, the SiO_2/SiN_x (300 nm/600 nm) was grown on the surface to passivate device. Owing to the high energy barrier of SiN_x layer, the gate leakage is suppressed to sub 1nA across the entire operation region, as shown in Fig. 2.

III. EXPERIMENTS AND RESULTS
A. CHARACTERIZATION OF DEGRADATION UNDER FORWARD AND REVERSE BIAS STRESS

To suppress the unintentional recovery during the measurement, spot-I_d [16] sense measurement is adopted instead of slow DC I/V sweep measurement to characterize the degradation as shown in Fig. 3. Prior to the stress, a pre-stress DC I–V sweep with V_g sweeps from −10V to 0V and $V_d = 0.1V$ is performed with the device (not drawn in Fig. 3) and serves as reference characteristic for the determination of the threshold voltage shift (ΔV_{th}). A stress voltage, $V_{gstress}$, is then applied on the device, an intermittent drain current I_d sensing at $V_{gmeasure}$ is monitored in
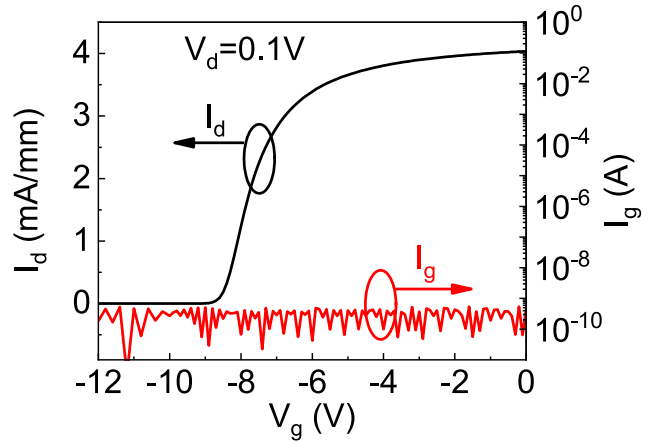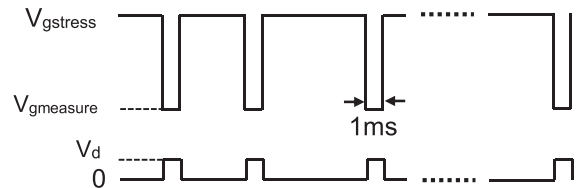
a preset log-incremental stress time to capture the degradation kinetics. Drain is biased at 0V during stress phase and 0.1V during sense phase. Measurement time is set to 1 millisecond as a trade-off between the gate lag effect [17] and the escaping of the fast recoverable border traps [18]. All the measurements are conducted on Keysight B1500A under room temperature (25°C). Note due to the limitation of Keysight B1500 software [19], the waveform in Fig. 3 needs to be constructed by a combination of multiple I/V-t sampling tests, and there is a ~2 seconds delay between 2 different tests, users need to switch on the "output bias hold" option to maintain the stress bias during the test delay, thus the stress time period cannot be set to less than 2 seconds. In this work, the minimum stress time was set to 5 seconds.

The spot-I_d sense measurement converts the I_d drop (ΔI_d) at a constant $V_{gmeasure}$ to ΔV_{th} by projecting ΔI_d to the fresh transfer characteristic, as shown in Fig. 4a. Note this conversion method is only accurate while the mobility and on-resistance remains unchanged before and after stress, which is the case on our device. Fig. 4 depicts a comparison between the transfer characteristics at the end of −13V 1000s (1ks) and +10V 1ks, it turns out the mobility and Ron do hardly changes in these 2 extreme cases, as shown in the inset of Fig. 4a, the max-gm value is the same for the two transfer characteristics, suggesting they possess the same mobility [20] and Ron. In addition, ΔV_{th} at different $V_{gmeasure}$ were calculated and compared with the max gm method extracted value, as shown in Fig. 4b. It is observed that $V_{gmeasure}$ selection has little impact on ΔV_{th} conversion,
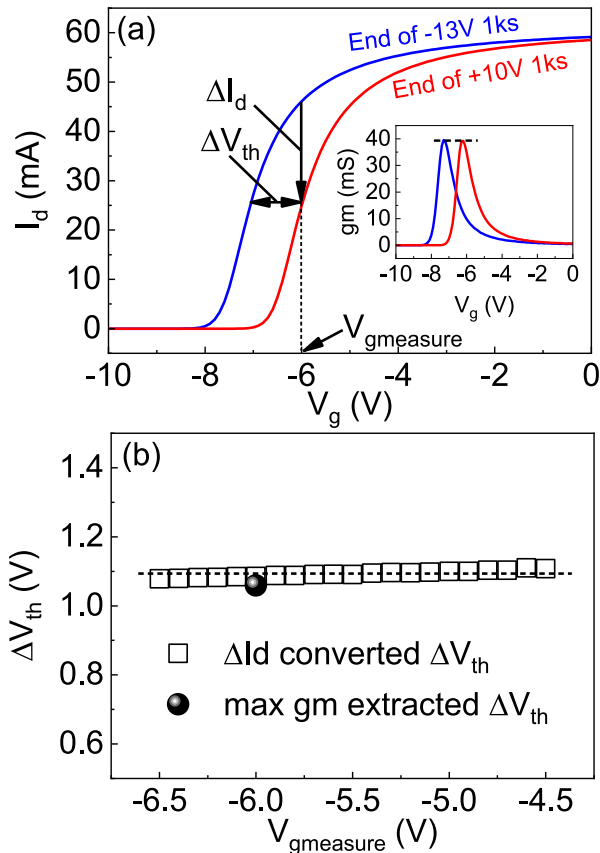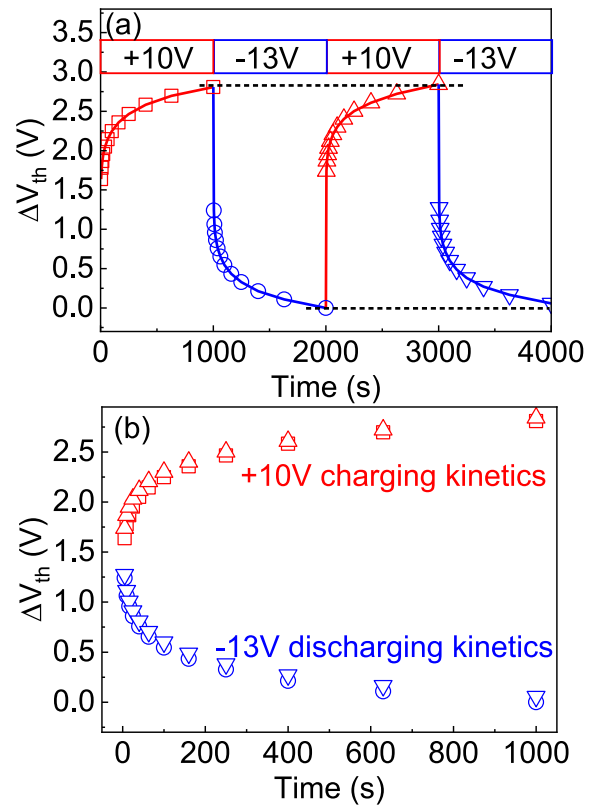
FIGURE 4. (a) Illustration of the $\Delta I_d \sim \Delta V_{th}$ conversion, the 2 transfer characteristics were measured at the end of $-13V$ 1ks (blue) and $+10V$ 1ks (red), respectively. The inset shows the gm value of the 2 transfer characteristics. (b) Comparison of ΔV_{th} converted from ΔI_d at different $V_{gmeasure}$ and extracted from max gm method.


FIGURE 5. (a) ΔV_{th} under $+10V/-13V$ alternating forward/reverse bias stress, the $+10V$ 1ks stress induced degradation is fully recoverable under $-13V$ 1ks; (b) $+10V/-13V$ exhibits the same charging/discharging kinetics, suggesting no extra traps were generated during forward/reverse bias stress.

and the converted ΔV_{th} is very close to the max gm method extracted value, further justifying the spot-I_d sense method.

A typical spot-I_d sense experiment results are given in Fig. 5. The device is subjected to a $+10V/-13V$ alternating stress, in each phase the stress time is set from 5s to 1ks. Fig. 5a shows ΔV_{th} reaches 2.81V after $+10V$ 1ks stress, and the degradation can be fully recovered after -13V 1ks. Note ΔV_{th} here is much larger than the I/V sweep measurement (Fig. 4b), as it contains fast recoverable border traps. Moreover, the stress and recovery kinetics in different cycles exhibit tiny difference, as illustrated in Fig. 5b, indicating there is no trap generation during forward/reverse bias stress up/down to $+10V/-13V$.

B. PRINCIPLES OF THE DTEP TECHNIQUE

The waveform of the proposed DTEP technique is depicted in Fig. 6. A spot Id sense measurement under high forward bias stress voltage, $V_{gstress}$, is firstly applied on the device to fill available border traps, stress time is set from 5s to 1ks. After the stress time reaches 1ks, V_g then steps down by a predefined ΔV_g gradually to discharge the available border traps until the last $V_{gdischarge}$ is met. The discharging

time for each $V_{gdischarge}$ is set from 5 seconds to 100 seconds to alleviating the charging effect under relatively high $V_{gdischarge}$ levels, as detailed in the explanation of principles of the DTEP technique.
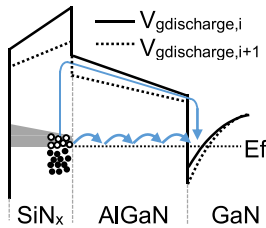
Fig. 7 illustrates the principles of DTEP technique to extract border traps' energy distribution. Considering the case of $V_{gdischarge}$ drops from $V_{gdischarge,i}$ to $V_{gdischarge,i+1}$, the fermi level E_f lowers down, accommodating a shaded region, where the filled border traps' energy is now above E_f. Given sufficient discharging time, all the border traps in the shaded region should be able to discharge, either by tunneling through the AlGaN barrier or via trap-assisted conduction [21]. By sweeping $V_{gdischarge}$ from the forwards bias stress level to the reverse bias, the density of border traps across the entire energy domain is achieved.

C. ENERGY DISTRIBUTION EXTRACTION

Note since the spatial distribution of border traps is not known, and traps located in AlGaN barrier and AlGaN/GaN interface could also induce ΔV_{th}, the concept of effective trap density is used in this work similarly to the early works [22], [23]. Traps are assumed to be at the SiN_x/AlGaN interface and the effective density is required to induce the same ΔV_{th} as that by the real spatially distributed traps spreading in the whole gate stack.
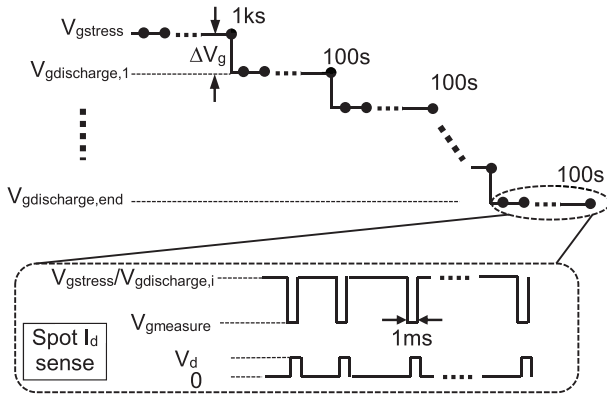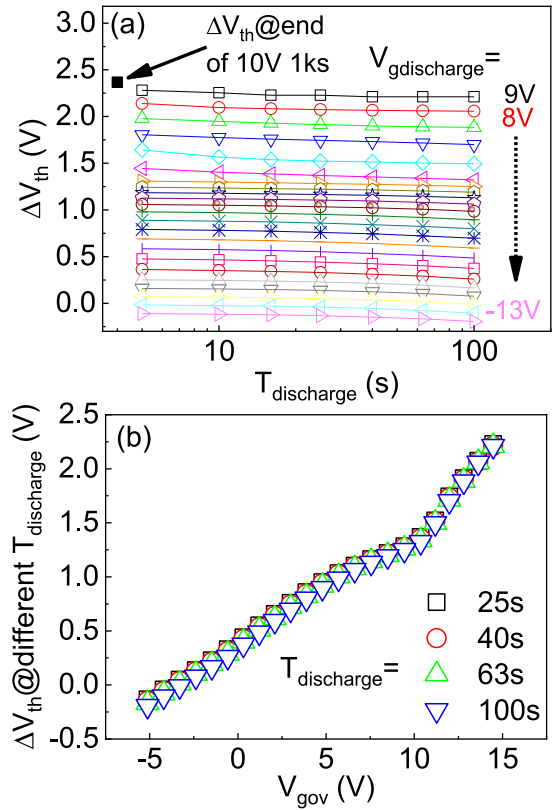
FIGURE 6. Test waveform of the DTEP technique.

FIGURE 7. Illustration of the principle of DTEP technique to extract border traps' energy distribution, the solid/dashed band diagram represent the energy band under $V_{gdischarge,i}/V_{gdischarge,i+1}$ respectively.

FIGURE 8. (a) Typical results of the DTEP technique. The slow down of ΔV_{th} decline after 25s indicates the majority of available border traps are discharged. (b) ΔV_{th} against V_{gov} at different $T_{discharge}$.

A typical test result of the DTEP technique is given in Fig. 8a. $V_{gstress} = +10V$, $V_{gdischarge}$ gradually lowers down from 9V to -13V at a constant step $\Delta V_g = 1V$. Note ΔV_g cannot be set too small in order to guarantee discharging is dominant during all $V_{gdischarge}$. We see ΔV_{th} reaches 2.37V after +10V 1ks stress. V_g then lowers down to $V_{gdischarge,1} = 9V$, ΔV_{th} starts to decrease due to the discharging of the border traps as explained before. As discharging time evolves, ΔV_{th} gradually decreases, as shown by the '□' in Fig. 8a. Note since the first discharging time is already 5s, there is an abrupt drop of ΔV_{th} from the last value of $V_{gdischarge,i}$ to the first value of $V_{gdischarge,i+1}$, and suggesting the majority of border traps locate close to the SiN$_x$/AlGaN interface and discharge within 5 seconds. After the discharging time $T_{discharge}$ reaches the predefined value (100 seconds here to avoid further trapping and guarantee the discharging process to be dominant), $V_{gdischarge}$ then keeps dropping and similar ΔV_{th} kinetics against $T_{discharg}$ is observed. By plotting the ΔV_{th} value in the end of the discharging time against the corresponding overdrive voltage $V_{gov} = V_g - V_{th}$, ΔV_{th} profile against V_{gov} can be obtained, as shown by the '▽' in Fig. 8b. The $\Delta V_{th} \sim V_{gov}$ profiles extracted at different discharging time are also plotted as a comparison in Fig. 8b, the negligible difference further indicates that 25~100 seconds is capable to discharge most available border traps.

To obtain the border traps' energy distribution, $\Delta V_{th} \sim V_{gov}$ needs to be converted to trap density against trap energy. As we use effective trap density at SiN$_x$/AlGaN

interface, the cumulative trap density N_{trap} can be obtained by

$$N_{trap} = \Delta V_{th} \cdot C_{SiN_x}/q \qquad (1)$$

where q is the basic electric charge and C_{SiNx} is the capacitance perunit area calculated by

$$C_{SiN_x} = \varepsilon_{SiN_x} \cdot \varepsilon_0 / T_{SiN_x} \qquad (2)$$

where ε_{SiNx} is the coefficient of SiN$_x$, ε_0 is vacuum dielectric constant and T_{SiNx} is the thickness of the SiN$_x$ dielectric layer. Assuming all the border traps above E_f is empty and below E_f is filled, the trap energy then equals to E_f thus its relation to V_{gov} can be obtained from TCAD simulations [24], as shown in the inset of Fig. 9a. Combining Equations 1&2 and $V_{gov} \sim E_c - E_{trap}$($E_c$ is the bottom of conduction band at SiN$_x$/AlGaN interface), the cumulative trap density $N_{trap} \sim E_c - E_{trap}$ distribution is calculated and shown in Fig. 9a. After obtaining N_{trap} distribution, density distribution D_{trap} can be derived from the first order differentiation on N_{trap}, as shown in Fig. 9b. Overall, in the range of $E_c - E_{trap}$ from -1.78eV to -0.26eV, D_{trap} becomes higher as E_{trap} approaching E_c. Moreover, two notable peaks are observed at $E_c - E_{trap} = -0.46$eV and -0.3eV, with the peak density of 2.91×10^{11} and 8.93×10^{11}cm^{-2}·eV^{-1} respectively.
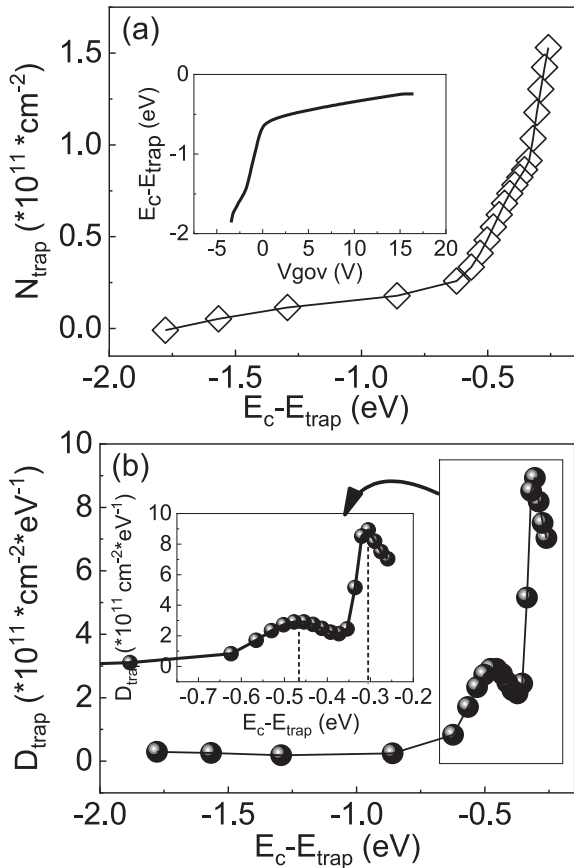
FIGURE 9. (a) Cumulative border traps' density N_{trap} against trap energy $E_c - E_{trap}$, the inset shows the conversion from V_{gov} to energy, which is obtained from TCAD simulation. (b) Energy distribution of border traps' density D_{trap} against trap energy Ec -Etrap, the inset enlarges the distribution plot in trap energy of [−0.75, −0.2] region for better observation.

FIGURE 10. (a) Effect of temperature on the energy distribution of D_{trap}. (b) An enlarged plot of D_{trap} energy distribution in trap energy range of [−0.7, −0.2] for clearer observation.

To test the robustness of the proposed technique, DTEP experiments are conducted under different temperatures. The extracted energy distribution results are shown in Fig. 10. We see although the overall trap density distribution becomes slightly higher as temperature rises, they exhibit the same shape, indicating the extracted energy distribution is of physical meaning and the proposed technique is robust against temperature. The overall slight higher trap density might be caused by the fact that, some inactive traps under room temperature, either due to a further location from SiN_x/AlGaN interface, or due to a high activation energy, become available to be involved (trapping/detrapping) within our experiment time domain under elevated temperatures.

IV. CONCLUSION

A discharging-based fast extraction method of energy distribution of border traps in AlGaN/GaN MIS-HEMT is proposed in this brief. The method adopts spot-I_d sense measurement with 1 millisecond measurement time to capture both fast and slow border traps. The experiment results show the overall border trap density, D_{trap}, becomes higher as E_{trap} approaching E_c, in the range of $E_c - E_{trap}$ from-1.78eV

to −0.26eV. Moreover, two notable peaks are observed at $E_c - E_{trap} = -0.46eV$ and −0.3eV, with the peak density of 2.91×10^{11} a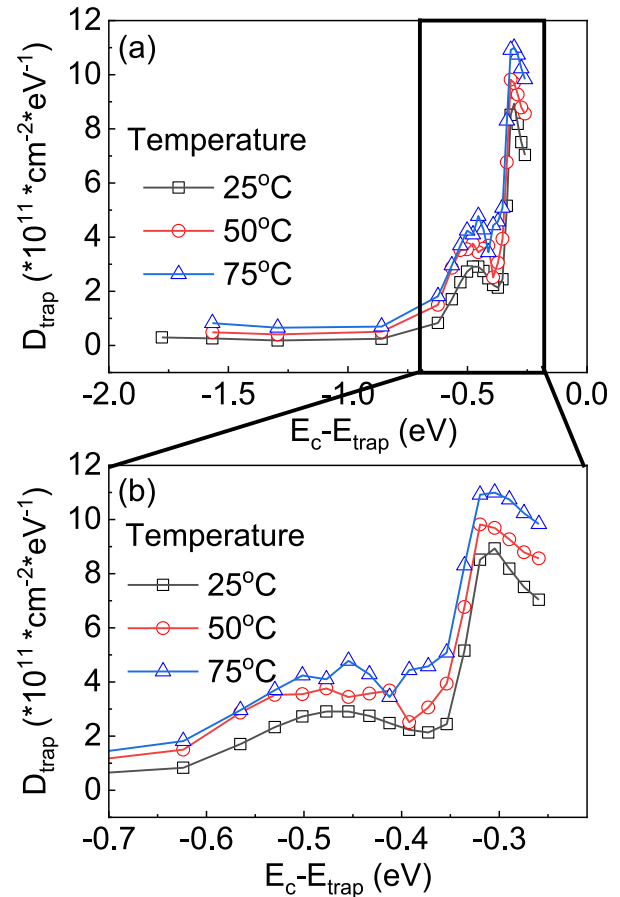nd $8.93 \times 10^{11} cm^{-2} \cdot eV^{-1}$ respectively. The method is of potential use for quick process screening and improvement of device performance and reliability.

REFERENCES

[1] N. Shigekawa, K. Shiojima, and T. Suemitsu, "Electroluminescence characterization of AlGaN/GaN high-electron-mobility transistors," *Appl. Phys. Lett.*, vol. 79, no. 8, pp. 1196–1198, 2001, doi: 10.1063/1.1398332.

[2] C. Zeng et al., "Reliability investigations of AlGaN/GaN HEMTs based on on-state electroluminescence characterization," *IEEE Trans. Device Mater. Rel.*, vol. 15, no. 1, pp. 69–74, Mar. 2015, doi: 10.1109/tdmr.2014.2360891.

[3] P. B. Klein, J. A. Freitas, Jr., S. C. Binari, and A. E. Wickenden, "Observation of deep traps responsible for current collapse in GaN metal–semiconductor field-effect transistors," *Appl. Phys. Lett.*, vol. 75, no. 25, pp. 4016–4018, 1999, doi: 10.1063/1.125523.

[4] P. B. Klein, S. C. Binari, J. A. Freitas, and A. E. Wickenden, "Photoionization spectroscopy of traps in GaN metal-semiconductor field-effect transistors," *J. Appl. Phys.*, vol. 88, no. 5, pp. 2843–2852, 2000, doi: 10.1063/1.1287127.

[5] D. V. Lang, "Deep-level transient spectroscopy: A new method to characterize traps in semiconductors," *J. Appl. Phys.*, vol. 45, no. 7, pp. 3023–3032, 1974, doi: 10.1063/1.1663719.

[6] T. Okino, M. Ochiai, Y. Ohno, S. Kishimoto, K. Maezawa, and T. Mizutani, "Drain current DLTS of AlGaN-GaN MIS-HEMTs," *IEEE Electron Device Lett.*, vol. 25, no. 8, pp. 523–525, Apr. 2004, doi: 10.1109/LED.2004.832788.

[7] Y. Liu, H. He, R. Chen, Y.-F. En, B. Li, and Y.-Q. Chen, "Analysis and simulation of low-frequency noise in indium-zinc-oxide thin-film transistors," *IEEE J. Electron Devices Soc.*, vol. 6, pp. 271–279, Jan. 2018, doi: 10.1109/jeds.2018.2800049.

[8] Y. Q. Chen *et al.*, "Effect of hydrogen on defects of AlGaN/GaN HEMTs characterized by low-frequency noise," *IEEE Trans. Electron Devices*, vol. 65, no. 4, pp. 1321–1326, Apr. 2018, doi: 10.1109/ted.2018.2803443.

[9] S. Li, Z. He, R. Gao, Y. Chen, Y. Liu, and Z. Zhu, "Time-dependent characteristics and physical mechanisms of AlGaN/GaN metal–insulator–semiconductor high electron mobility transistors under different bias conditions," *J. Phys. D Appl. Phys.*, vol. 52, no. 48, 2019, Art. no. 485106, doi: 10.1088/1361-6463/ab3d52.

[10] M. Silvestri, M. J. Uren, N. Killat, D. Marcon, and M. Kuball, "Localization of off-stress-induced damage in AlGaN/GaN high electron mobility transistors by means of low frequency 1/f noise measurements," *Appl. Phys. Lett.*, vol. 103, no. 4, pp. 40–46, 2013, doi: 10.1063/1.4816424.

[11] A. N. Tallarico, E. Sangiorgi, C. Fiegna, P. Magnone, G. Barletta, and A. Magri, "Modeling spatial and energy oxide trap distribution responsible for NBTI in p-channel power U-MOSFETs," in *Proc. ISPSD*, 2015, pp. 153–156, doi: 10.1109/ISPSD.2015.7123412.

[12] X. F. Zheng, W. D. Zhang, B. Govoreanu, J. F. Zhang, and J. V. Houdt, "A discharge-based multi-pulse technique (DMP) for probing electron trap energy distribution in high-k materials for flash memory application," in *IEDM Tech. Dig.*, 2009, pp. 1–4, doi: 10.1109/IEDM.2009.5424403.

[13] S. W. M. Hatta *et al.*, "Energy distribution of positive charges in gate dielectric: Probing technique and impacts of different defects," *IEEE Trans. Electron Devices*, vol. 60, no. 5, pp. 1745–1753, May 2013, doi: 10.1109/ted.2013.2255129.

[14] J. Ma *et al.*, "Energy distribution of positive charges in $Al_2O_3/GeO_2/Ge$ pMOSFETs," *IEEE Electron Device Lett.*, vol. 35, no. 2, pp. 160–162, Feb. 2014, doi: 10.1109/led.2013.2295516.

[15] R. Gao *et al.*, "A discharge-based pulse technique for probing the energy distribution of positive charges in gate dielectric," *IEEE Trans. Semicond. Manuf.*, vol. 28, no. 3, pp. 221–226, Aug. 2015, doi: 10.1109/TSM.2015.2407909.

[16] C. D. Young *et al.*, "Ultra-short pulse current–voltage characterization of the intrinsic characteristics of high-κ devices," *Jpn. J. Appl. Phys.*, vol. 44, no. 4B, pp. 2437–2440, 2005, doi: 10.1143/JJAP.44.2437.

[17] O. Mitrofanov and M. Manfra, "Mechanisms of gate lag in GaN/AlGaN/GaN high electron mobility transistors," *Superlattices Microstructures*, vol. 34, nos. 1–2, pp. 33–53, 2003, doi: 10.1016/j.spmi.2003.12.002.

[18] P. Lagger, A. Schiffmann, G. Pobegen, D. Pogany, and C. Ostermaier, "Very fast dynamics of threshold voltage drifts in GaN-based MIS-HEMTs," *IEEE Electron Device Lett.*, vol. 34, no. 9, pp. 1112–1114, Sep. 2013, doi: 10.1109/led.2013.2272095.

[19] I. Keysight, *Agilent EasyEXPERT User's Guide*, vol. 1, 1st ed. Santa Rosa, CA, USA: Keysight Inc., pp. 2.21–2.22, 2014.

[20] P. Ren *et al.*, "Understanding charge traps for optimizing Si-passivated Ge nMOSFETs," in *VLSI Symp. Tech. Dig.*, 2016, pp. 1–2, doi: 10.1109/VLSIT.2016.7573367.

[21] M. Meneghini *et al.*, "Negative bias-induced threshold voltage instability in GaN-on-Si power HEMTs," *IEEE Electron Device Lett.*, vol. 37, no. 4, pp. 474–477, Apr. 2016, doi: 10.1109/LED.2016.2530693.

[22] J. F. Zhang, I. S. Al-Kofahi, and G. Groeseneken, "Behavior of hot hole stressed SiO_2/Si interface at elevated temperature," *J. Appl. Phys.*, vol. 83, no. 2, pp. 843–850, 1998, doi: 10.1063/1.366766.

[23] D. J. Dimaria, "The properties of electron and hole traps in thermal silicon dioxide layers grown on silicon," in *Proc. Phys. SiO Interfaces*, pp. 160–178, Mar. 1978, doi: 10.1016/B978-0-08-023049-8.50034-8.

[24] Y. Shi *et al.*, "An extraction method for the interface acceptor distribution of GaN MOS-HEMT," *IEEE Trans. Electron Devices*, vol. 66, no. 10, pp. 4164–4169, Oct. 2019, doi: 10.1109/TED.2019.2936509.